IEEE Access
Multidisciplinary | Rapid Review | Open Access Journal

Received October 22, 2019, accepted November 3, 2019, date of current version November 15, 2019.

Digital Object Identifier 10.1109/ACCESS.2019.2952073

Bandwidth Extension of Planar Microstrip-to-Waveguide Transition by Controlling Transmission Modes Through Via-Hole Positioning in Millimeter-Wave Band

NGUYEN THANH TUAN, (Member, IEEE), KUNIO SAKAKIBARA, (Senior Member, IEEE), AND NOBUYOSHI KIKUMA, (Senior Member, IEEE)

Department of Electrical and Mechanical Engineering, Nagoya Institute of Technology, Nagoya 466-8555, Japan

Corresponding author: Kunio Sakakibara (sakaki@nitech.ac.jp)

ABSTRACT This paper presents a design technique to achieve a broadband planar microstrip-to-waveguide transition in a millimeter-wave (mmWave) band. In the conventional planar microstrip-to-waveguide transition, via holes are located around the rectangular waveguide and microstrip line to prevent power leakage due to the generation of a multi-transmission mode. Therefore, a single-transmission mode is dominant at the input port of the transition, with a narrow bandwidth of the single resonance. In the broadband planar microstrip-to-waveguide transition, via-hole positioning is utilized to add inductance to constrain the predominance of the single-transmission mode at the input port of the transition. The double-resonant frequency yielded by excitation of the grounded coplanar waveguide transmission mode and parallel plate transmission mode is obtained by controlling the positions of holes adjacent to the microstrip line. Moreover, to simplify the structure and meet the requirement of high assembly accuracy in fabrication, two holes adjacent to the microstrip line are maintained, but the remaining holes are replaced by a choke structure that performs the equivalent function to the via-hole arrangement. The influences of the multi-transmission mode and choke structure on the characteristics are investigated by electromagnetic analysis, and the feasibility is confirmed by experiments in this work. A double-resonant frequency and a broad bandwidth of 10.6 GHz (13.8%) are obtained. The measured results of the broadband planar microstrip-to-waveguide transition using via-hole positioning show an insertion loss of 0.41 dB at the center frequency of 76.5 GHz.

INDEX TERMS Microwave and millimeter-wave circuits, broadband, microstrip transition, waveguide transition, multi-transmission mode.

I. INTRODUCTION

MILLIMETER-WAVE (mmWave) technologies have been applied in various applications of broadband high-speed wireless communication systems, such as fixed wireless access [1], wireless LAN [2], 5G antenna systems [3] or high angular resolution automotive radars [4]–[7]. The next generation of ultra-wideband (UWB) automotive radar requires a wider frequency bandwidth [8]. Antennas in mmWave systems with a high gain and a narrow beam even when the physical size of the antenna aperture is very small could be developed. Such antennas are appropriate for meeting the demand for high traffic capacities and beam steering capabilities in mmWave applications. Some mmWave applications have been studied and commercialized on the market. Antennas for these products are designed depending on the specifications required for the systems such as performance, physical size or production cost. Several types of antennas have been developed for mmWave systems, including dielectric lens antennas [9], folded reflector antennas [10], slot antennas [11], [12], etc. The microstrip array antenna is one of the most attractive options for realizing a low cost and a low profile, which can be easily integrated into the RF circuit of mmWave devices.

Techniques for integrating a microstrip array antenna into an RF circuit were developed by using a microstrip-to-waveguide transition. The performances of microstrip array antennas fed by microstrip-to-waveguide transitions were

The associate editor coordinating the review of this manuscript and approving it for publication was Kwok L. Chung.

reported in [13], [14]. However, to meet the demand of a feeding line for a broadband antenna, the design techniques for a broadband transition need to be enhanced. In the usual configuration of the transition, the oscillating signals are transmitted into the rectangular waveguide through microstrip lines. The typical transitions from a microstrip line to a waveguide are classified as longitudinal and vertical transitions. The transitions of the ridge waveguide [15], quasi-Yagi [16], and planar waveguide [17] types are examples of longitudinal transitions from a microstrip line to a waveguide. However, in current PCB designs, the antenna layer is commonly parallel to the RF circuit on the back, and they are connected by a perpendicular waveguide. Consequently, vertical transitions have been proposed, such as probe feeding [18] and slot coupling [19] transitions. Various types of broadband microstrip-to-waveguide transitions have been developed for multilayer planar circuits in the mmWave band [20]–[25]. However, the structures were quite complex because they were designed by combining substrate integrated waveguide (SIW) and microstrip line (ML) techniques.

The probe feeding transition has a wideband characteristic; however, a quarter-wavelength metal short block on top of the substrate is necessary to obtain sufficient coupling between the microstrip line and the waveguide. This results in an increase in the transition size. The probe feeding transition has been replaced by the slot coupling transition, which is composed of two-layer dielectric substrates without a metal short block. The electromagnetic field of the microstrip line is coupled to the matching patch through the excitation of a slot. To simplify the structure of the microstrip-to-waveguide transition, a planar transition composed of a single dielectric substrate was proposed [26]–[31]. Via holes are arranged around the waveguide aperture to prevent power leakage from travelling in the parallel plate transmission line formed in the dielectric substrate. However, the conventional planar microstrip-to-waveguide transition operates over a quite narrow frequency bandwidth in terms of the mmWave band. Therefore, a design technique to extend the bandwidth of the planar microstrip-to-waveguide transition is necessary.

This study proposes a technique of using multi-transmission mode excitation to form a double-resonant structure. The multi-modes of the grounded coplanar waveguide (G-CPW) and parallel plate modes can be generated and controlled based on the via-hole locations at both sides of the microstrip line. As a result, a broadband planar microstrip-to-waveguide transition is obtained by the formation of a double-resonant frequency when the transition input is dominated by different transmission excitations. Subsequently, a combination of via holes controlling the multi-transmission mode and a choke structure are proposed to simplify the structure of the planar microstrip-to-waveguide transition. Compared to the performance of the transition with via-hole arrangement, the transition with a choke structure shows similar reflection and transmission characteristics even with the simple structure. Moreover, the reliability of the simulated results is confirmed by measured results in this paper.

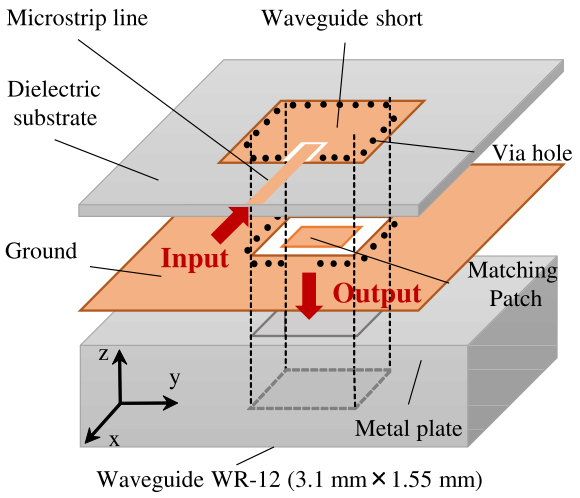

FIGURE 1. Configuration of the planar microstrip-to-waveguide transition.

In this paper, the structures of the broadband planar microstrip-to-waveguide transitions with the proposed via-hole arrangement and choke structure are described in section II. The simulation investigation on double resonance is presented in section III, in which the characteristics of the broadband microstrip-to-waveguide transition depending on the parameters of the via holes and choke structure are numerically investigated by electromagnetic analysis using the finite element method [32]. In section IV, the feasibility of the proposed design techniques is confirmed by the experimental performance. Conclusions are then presented in Section V.

II. BROADBAND PLANAR MICROSTRIP-TO-WAVEGUIDE TRANSITION

A planar microstrip-to-waveguide transition is a simple structure; it is only a dielectric substrate on a metal plate. The configuration of the planar microstrip-to-waveguide transition in the millimeter-wave band is illustrated in Fig. 1. The transition is composed of a single-layer dielectric substrate with conductor patterns on metal plates and an open-ended rectangular waveguide (WR-12, 3.1 mm × 1.55 mm). Using etching technology, a matching patch is formed at the center of the waveguide profile on the lower plane of the dielectric substrate. On the upper plane of the dielectric substrate, a microstrip line is inserted into a waveguide short. Consequently, when the signal from the microstrip line transmits to the transition, the electromagnetic fields at the end of the line will be electrically coupled to the matching patch on the lower plane of the substrate. Then, the electromagnetic power transmits to the rectangular waveguide. These phenomena are created by the electromagnetic fields of the quasi-TEM transmission mode of the microstrip line coupled to the magnetic field of the TM_{01} dominant mode of the patch antenna, as illustrated in Fig. 2. The relationships between the parameters and the bandwidth were investigated to determine the optimum parameters of the transition [28]. The quality

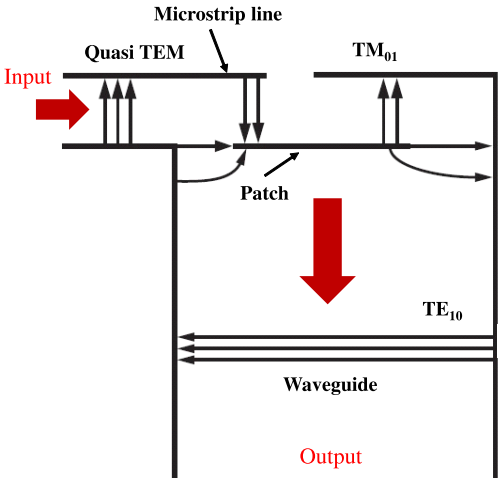

FIGURE 2. Transmission mode in the planar microstrip-to-waveguide transition.

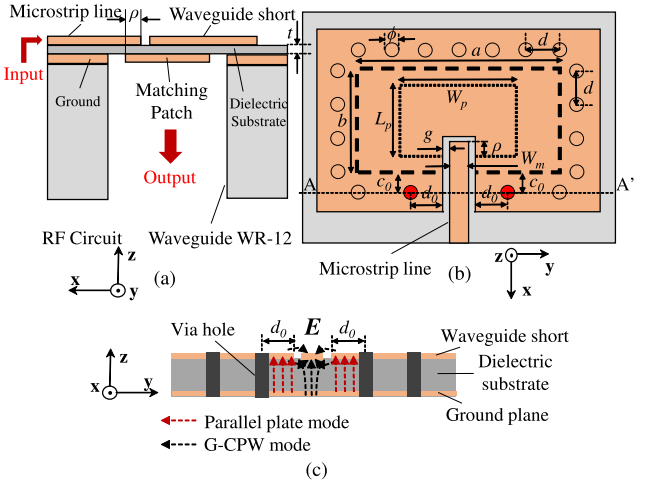

FIGURE 3. Cross-sectional views along with the parameters of the broadband planar microstrip-to-waveguide transition. (a) xz plane. (b) xy plane. (c) Propagation mode in the AA' plane.

factor of the power transmitted into the waveguide Q_{WG} is expressed as follows:

$$Q_{WG} = \frac{15\omega\pi^2\varepsilon_0\varepsilon_e L_e b}{4t}\frac{1}{\sqrt{1-(\frac{\lambda_g}{2a})^2}}\frac{C}{(sinC)^2} \quad (1)$$

where ω and ε_e are the angular frequency and effective permittivity of the dielectric substrate. C is a constant coefficient of 1.666. In the conventional microstrip-to-waveguide transition, the frequency bandwidth is quite narrow due to the high Q factor and single-resonant frequency of the transition. Therefore, the design technique of multi-transmission mode excitation for realizing the double-resonant frequency of the transition is proposed and discussed in this section.

A. PROPOSED VIA-HOLE ARRANGEMENT FOR REALIZING THE MULTI-TRANSMISSION MODE

This section describes a simple but effective technique for enhancing the frequency bandwidth of a planar microstrip-to-waveguide transition. Cross-sectional views of the broadband planar microstrip-to-waveguide transition along with the geometrical parameters are shown in Fig. 3. A dielectric substrate (relative permittivity $\varepsilon_r = 2.2$, loss tangent $\tan\delta = 0.001$ and thickness $t = 0.127$ mm) is located at the aperture of the waveguide, as presented in Fig. 3(a). The end of the microstrip line overlaps the matching patch with an insertion length ρ. Impedance matching can be obtained by controlling the insertion length ρ of the microstrip line. Fig. 3(b) illustrates an upper view and the geometrical parameters of the broadband microstrip-to-waveguide transition. The dashed line and the dotted line indicate the patterns of the waveguide profile and matching patch, respectively. The microstrip line width is set to $W_m = 0.3$ mm (characteristic impedance of $Z_0 = 60\ \Omega$). The gap g between the microstrip line and the waveguide short equals 0.1 mm. The resonant frequencies of the transition can be controlled by adjusting the patch length L_p of the matching patch. The patch length and patch width are respectively optimized as $L_p = 1.12$ mm and $W_p = 1.8$ mm. Adequate impedance matching of the transition is obtained by optimizing the value of the insertion length to $\rho = 0.16$ mm.

In the conventional transition, via holes are located close to the microstrip line to prevent higher-order modes, enabling the G-CPW mode to dominate at the input port of the microstrip line insertion in the waveguide short. However, in the design of the broadband planar microstrip-to-waveguide transition, two holes adjacent to the microstrip line are utilized as added inductance to constrain the predominance of the single-transmission mode at the input port. The influences of these two holes can be controlled by the distance d_0 between the via holes and the edge of the waveguide short and the distance c_0 between the via holes and the waveguide profile.

By choosing appropriate values of d_0 and c_0, the G-CPW mode is no longer dominant at the input port, and an additional transmission mode exists in the area between the via holes spaced by d_0 in addition to the electric field distributions of the G-CPW mode, as illustrated in Fig. 3(c). This is considered as a parallel plate mode formed by coplanar strips and the ground plane at the upper and lower sides of the dielectric substrate. The multi-transmission mode is effective in extending the frequency bandwidth of the proposed transition. On the other hand, the structure of the transition can give rise to various resonances under the dominant excitation of particular transmission modes at different frequencies. In this proposed structure, a double-resonant frequency is generated for broadband operation when the G-CPW mode excites the patch antenna and the parallel plate mode excites the slot between the waveguide profile and the patch at different frequencies. Table 1 summarizes the optimum parameters of the broadband planar microstrip-to-waveguide transition. The distances d_0 and c_0 are optimized as 0.5 mm and 0.28 mm, respectively. The pitch sizes d of the

TABLE 1. Parameters of the broadband planar microstrip-to-waveguide transition.

Parameters	Values (mm)
Transition dimensions (length × width × height)	2.8×4.4 ×0.163
Broad wall length a of waveguide	3.1
Narrow wall length b of waveguide	1.55
Patch length L_p	1.12
Patch width W_p	1.8
Insertion length ρ of microstrip line	0.16
Thickness t of dielectric substrate	0.127
Width W_m of microstrip line	0.3
Gap g between microstrip line and waveguide short	0.1
Diameter ϕ of via holes	0.2
Pitch size d of via holes	0.516
Distance d_0 between via holes and edge of waveguide short	0.5
Distance c_0 between via holes and waveguide profile	0.28

via holes are equally 0.516 mm. The formation of the multi-transmission mode by via-hole positioning is investigated by numerical simulations.

B. CHOKE STRUCTURE

The via-hole arrangement reduces the transmission loss of the planar microstrip-to-waveguide transition. However, disadvantages of via holes could be encountered in fabrication. The characteristics of the planar microstrip-to-waveguide transition could be unexpectedly degraded due to the tolerance of via holes during mechanical machining. To reduce the influence of the fabrication tolerance and simplify the structure of the planar microstrip-to-waveguide transition, a drastic reduction of the number of via holes is proposed in this section. The two via holes adjacent to the microstrip line are maintained to control the multi-transmission mode at the input port, and the remainder of the via holes are replaced by a choke structure [30].

The distance C of the choke on the waveguide short from the waveguide profile is examined to optimize the choke structure, as shown in Fig. 4(a). The choke structure plays the same role as the via-hole arrangement in preventing leakage through the parallel plate transmission line between the waveguide short and ground plane. To create an equivalent short circuit along with the waveguide profile, a pattern edge equivalent to an open circuit is formed with a distance of $C = \lambda_g/4$ (λ_g: wavelength in a dielectric substrate) from the waveguide profile, as shown in Fig. 4(b).

C. BROADBAND CHARACTERISTICS UNDER DOUBLE-RESONANT FREQUENCY

The simulated reflection characteristics of the conventional planar microstrip-to-waveguide transition and proposed broadband planar microstrip-to-waveguide transition are shown in Fig. 5. A single-resonant frequency of the patch antenna due to excitation of the G-CPW transmission mode was observed in the conventional transition. In the broadband

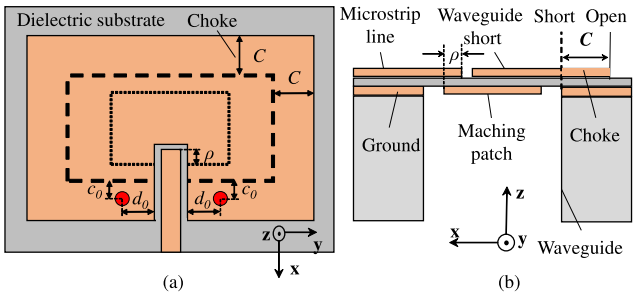

FIGURE 4. The replacement of via holes by a choke structure. (a) xy plane. (b) xz plane.

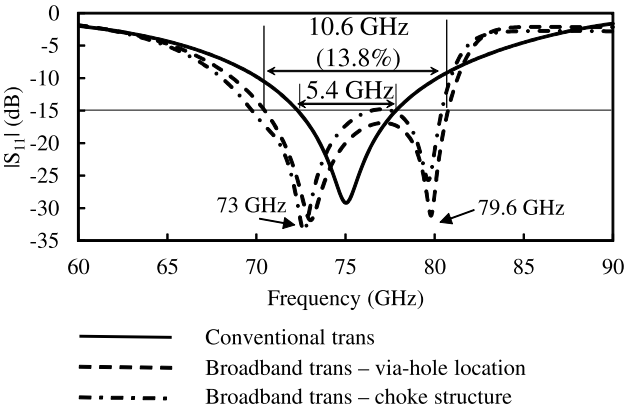

FIGURE 5. Simulated reflection characteristics of the conventional and broadband planar microstrip-to-waveguide transitions.

planar microstrip-to-waveguide transition, a double-resonant frequency was obtained at 73 GHz and 79.6 GHz when via holes were located at $d_0 = 0.5$ mm, with $c_0 = 0.28$ mm and an insertion length of the microstrip line of $\rho = 0.16$ mm. The bandwidth of reflection lower than -15 dB is enhanced to 10.6 GHz (13.8%) ($|S_{11}| = -15$ dB) due to the double resonance compared to the value of 5.4 GHz (7.2%) for the conventional transition. When via holes are replaced by the choke structure with the choke length C approximately set to a quarter-wavelength in the dielectric substrate, $C = 0.65$ mm, the reflection characteristic of the broadband planar microstrip-to-waveguide transition with the choke structure is similar to that with the proposed via-hole arrangement, as presented in Fig. 5.

To clearly understand the influences of the multi-transmission mode on the transition characteristics, an investigation based on a parametric study of the positioning parameters (d_0 and c_0) of the two via holes adjacent to the microstrip line and choke length C is conducted and discussed in the next section.

III. SIMULATION INVESTIGATION ON DOUBLE RESONANCE

A. PROPOSED VIA-HOLE ARRANGEMENT

This section describes the numerical investigations of the broadband microstrip-to-waveguide transition characteristics

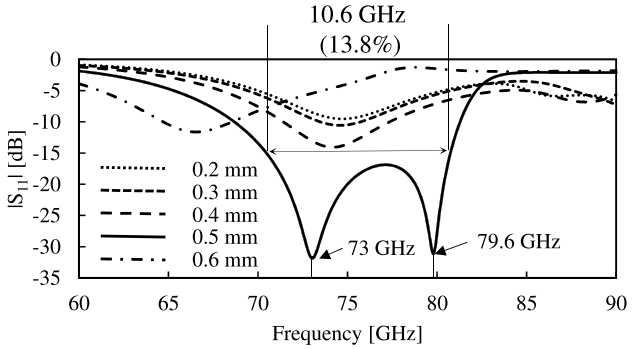

FIGURE 6. Reflection characteristics of the broadband planar microstrip-to-waveguide transition depending on d_0.

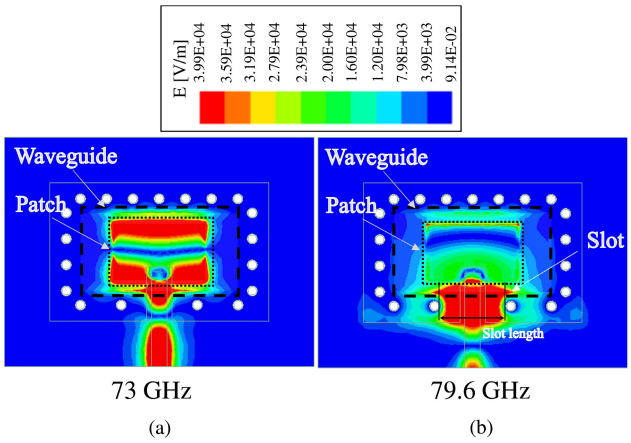

FIGURE 7. Electric field distributions in the dielectric substrate of the broadband planar microstrip-to-waveguide transition with the proposed via-hole arrangement. (a) 73 GHz. (b) 79.6 GHz.

depending on the multi-transmission mode based on the via-hole arrangement. The reflection characteristics of the transition depending on d_0 are investigated by varying d_0 from 0.2 mm to 0.6 mm with a step of 0.1 mm, as shown in Fig. 6. d_0 is set to 0.5 mm for multi-transmission mode operation at the input port of the transition, which results in a double-resonant frequency appearing at 73 GHz and 79.6 GHz due to the excitation of two transmission modes. The lower resonant frequency of 73 GHz is created by the patch resonance excited by the G-CPW mode; the higher resonant frequency of 79.6 GHz is formed by the parallel plate mode exciting the slot between the waveguide wall and patch antenna, as shown in Fig. 7. The frequency bandwidth is widened to 10.6 GHz for reflection levels lower than −15 dB.

In the cases of via-hole positions close to the microstrip line ($d_0 = 0.2$ mm, 0.3 mm, 0.4 mm) or far from the microstrip line ($d_0 = 0.6$ mm), the electrical function of the via holes cannot prevent the dominance of single-transmission mode excitation, resulting in a single-resonant frequency of the transition. For instance, the G-CPW mode is dominant when via holes are located close to the microstrip line, and the parallel plate mode is the dominant excitation when via holes are located far from the microstrip line.

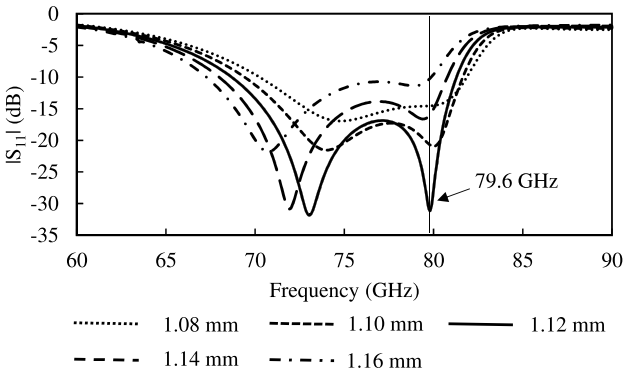

FIGURE 8. Reflection characteristics of the broadband planar microstrip-to-waveguide transition depending on L_p.

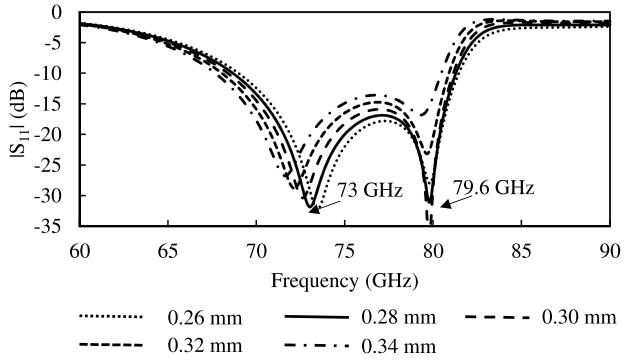

FIGURE 9. Reflection characteristics of the broadband planar microstrip-to-waveguide transition depending on c_0.

Therefore, by choosing an appropriate value of d_0, the multi-transmission mode can be propagated at the input port of the transition, and a double-resonant frequency can be obtained by multi-mode excitation.

To ensure the realization of patch resonance, the patch length L_p is investigated to assess the change in resonant frequencies. As shown in Fig. 8, the lower resonant frequencies are shifted to lower frequencies with increasing L_p, while higher resonant frequencies remain unchanged with the variation of L_p. This means that the G-CPW mode excites the different structures of the patch, which will result in different resonant frequencies. The higher resonant frequencies are due to the slot resonance; they are, of course, not affected by the patch structure.

The reflection characteristics of the transition depending on the distance c_0 between via holes and the waveguide profile are presented in Fig. 9. c_0 is assessed in the range from 0.26 mm to 0.34 mm with a step of 0.02 mm. When c_0 is gradually extended, the lower resonant frequencies are slightly shifted to lower values, but the higher resonant frequencies remain at 79.6 GHz. However, the reflection levels $|S_{11}|$ at the higher resonant frequencies decrease following the expansion of c_0. This indicates that the impedance matching of the coupling to the slot could be controlled by changing c_0. c_0 is optimized as 0.28 mm so that the reflection level $|S_{11}|$ is below −30 dB at 79.6 GHz.

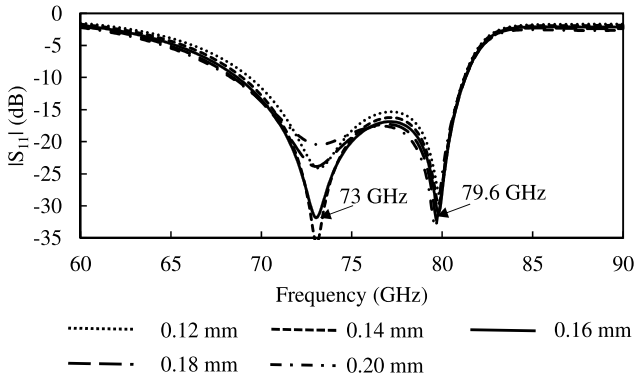

FIGURE 10. Reflection characteristics of the broadband planar microstrip-to-waveguide transition depending on ρ.

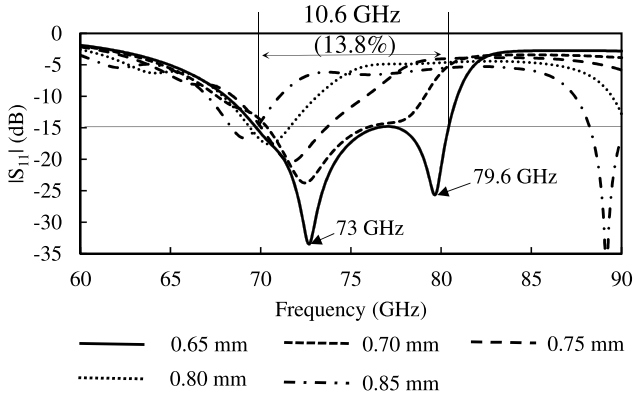

FIGURE 11. Reflection characteristics of the broadband planar microstrip-to-waveguide transition depending on choke length *C*.

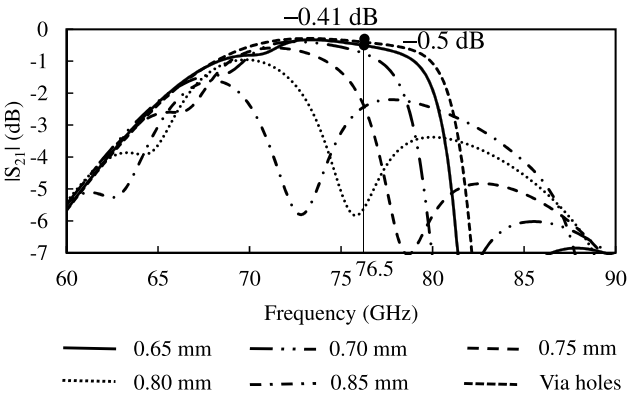

FIGURE 12. Transmission characteristics of the broadband planar microstrip-to-waveguide transition depending on choke length *C* compared to that with via-hole arrangement.

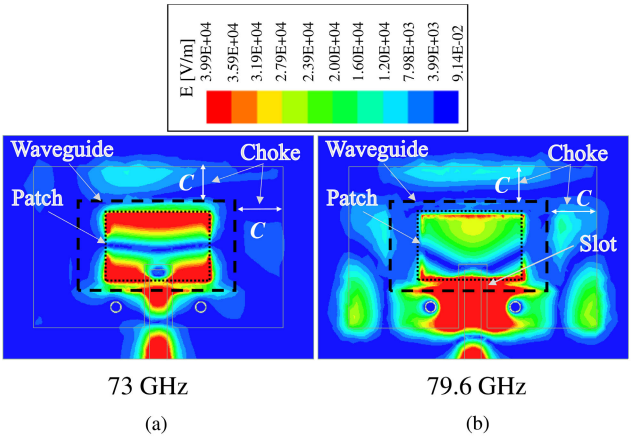

FIGURE 13. Electric field distributions in the dielectric substrate of the broadband planar microstrip-to-waveguide transition with the choke structure. (a) 73 GHz. (b) 79.6 GHz.

Moreover, impedance matching of the patch resonance can be obtained by controlling the insertion length ρ, as presented in Fig. 10. ρ is optimized as 0.16 mm so that the reflection level $|S_{11}|$ of the patch resonance is below -30 dB at 73 GHz.

Consequently, by optimizing the values of d_0, c_0, L_p and ρ, the input port of the broadband transition works over the multi-transmission mode of the G-CPW mode and parallel plate mode. The excitation of each mode at different frequencies results in the double resonance of the transition. The frequency bandwidth is enhanced approximately two-fold to 10.6 GHz (13.8%) compared to the conventional one of 5.4 GHz (7.2%) due to the formation of double resonance.

B. CHOKE STRUCTURE

In the broadband microstrip-to-waveguide transition using the choke structure, via holes are replaced by the choke structure. The reflection and transmission characteristics of the broadband planar microstrip-to-waveguide transition depending on the choke length C are presented in Figs. 11 and 12. When the choke length C is approximately set to a quarter-wavelength in the dielectric substrate, $C = 0.65$ mm, a reflection characteristic similar to that in the broadband microstrip-to-waveguide transition with the proposed via-hole arrangement is obtained, with double resonant frequencies at 73 GHz and 79.6 GHz.

By applying a choke structure, the waveguide short and ground plane are electrically connected along the waveguide profile due to the formation of an equivalent short circuit. Therefore, electromagnetic fields are mostly transmitted into the waveguide. Some electric field is observed in the choke structure because the choke works when it resonates from the edge of the waveguide short for an open circuit to the waveguide profile for a short circuit, as presented in Fig. 13. Therefore, the insertion loss is slightly increased compared with the transition with via-hole arrangement, as shown in Fig. 12. The insertion loss of the transition with the choke structure is 0.5 dB at 76.5 GHz, compared to 0.41 dB for the transition with via-hole arrangement. However, the choke structure still has advantages despite its simple structure. The feasibilities of the broadband planar microstrip-to-waveguide transitions with the proposed via-hole arrangement and choke structure are confirmed by their experimental performances in the next section.

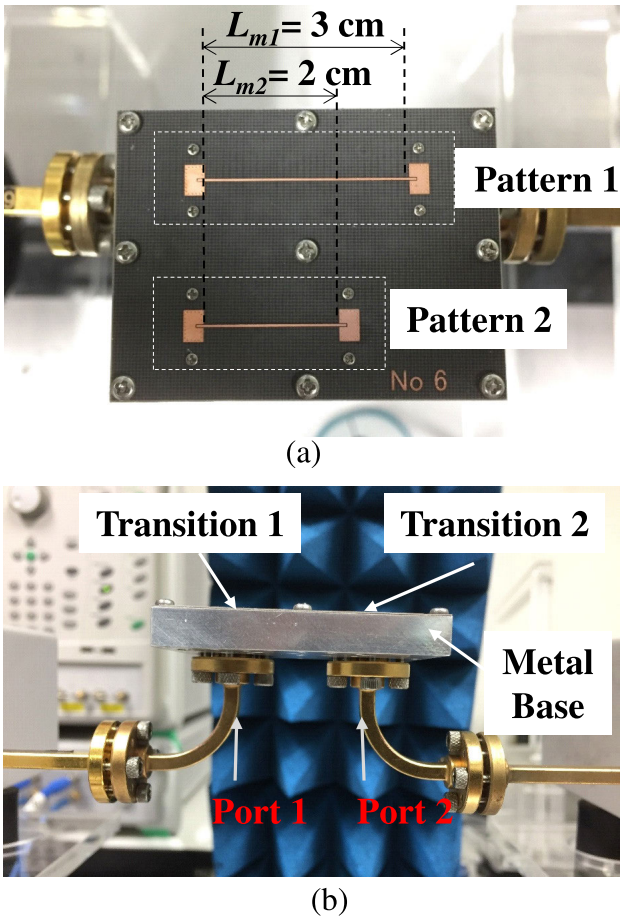

FIGURE 14. Experimental setup. (a) Upper view. (b) Side view.

IV. EXPERIMENTAL PERFORMANCES

Measurements are conducted to validate the reliability of the proposed techniques. An experiment is set up as shown in Fig. 14. Two patterns are laid out on a dielectric substrate. Each pattern is composed of two broadband planar microstrip-to-waveguide transitions with the same parameters, and they are connected by microstrip lines with different lengths, as shown in Fig. 14(a). Each transition is connected to a port of a vector network analyser (VNA) through a rectangular waveguide to measure the reflection and transmission characteristics, as shown in Fig. 14(b). Measurement of the $|S_{11}|$ and $|S_{21}|$ parameters is conducted using a gate function in the time domain [33]. In the time domain gating, a region of interest in a portion of the time domain is selected; gating removes unwanted responses, and the result is displayed in the frequency domain. Gating can be considered as a time domain reaction multiplier with a valuable mathematical function that corresponds to the area of interest. The controlled time domain function can then be converted to show the frequency response without the effect of the other responses in time. Therefore, the multi-reflected wave can be suppressed in the measurement.

The microstrip line lengths of pattern 1 and pattern 2 are set to $L_{m1} = 3$ cm and $L_{m2} = 2$ cm, respectively.

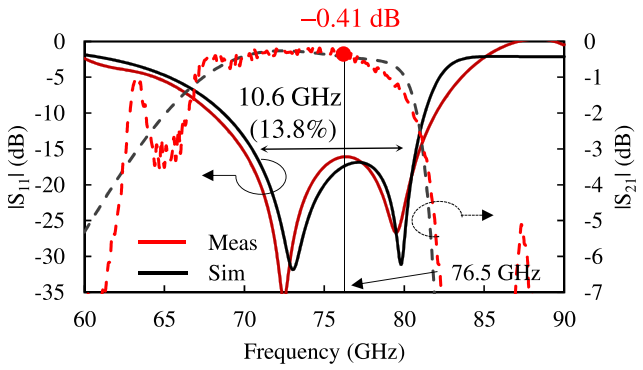

FIGURE 15. Measured and simulated $|S_{11}|$ and $|S_{21}|$ of the broadband microstrip-to-waveguide transition with the proposed via-hole arrangement.

From the difference in the measured results of pattern 1 and pattern 2, the transmission loss per centimeter of the microstrip line was estimated. The real insertion loss of the broadband microstrip-to-waveguide transition could be deduced by subtracting the loss of the microstrip line as follows:

$$S_{21} = \frac{S'_{21} - L_{m1}|(S'_{21} - S''_{21})|}{2} \tag{2}$$

where S_{21} is the actual measured insertion loss of the transition. S'_{21} and S''_{21} indicate the measured transmission losses of pattern 1 and pattern 2, respectively. $|(S'_{21} - S''_{21})|$ represents the transmission loss of the microstrip line in 1 cm. In this measurement, the transmission loss of the microstrip line was measured as 0.35 dB/cm.

The measured and simulated $|S_{11}|$ and $|S_{21}|$ of the broadband microstrip-to-waveguide transition with the proposed via-hole arrangement are presented in Fig. 15. Solid lines and dashed lines represent the $|S_{11}|$ and $|S_{21}|$ characteristics, respectively. The reflection characteristics show agreement between the measured and simulated results in which the measured result exhibits a double-resonant frequency at 72.8 GHz and 79.5 GHz and a broad frequency bandwidth of 10.6 GHz (13.8%) at $|S_{11}| = -15$ dB. The measured insertion loss at the center frequency of 76.5 GHz is 0.41 dB.

In addition, the measured and simulated $|S_{11}|$ and $|S_{21}|$ of the broadband microstrip-to-waveguide transition with the choke structure are presented in Fig. 16. Solid lines and dashed lines represent the $|S_{11}|$ and $|S_{21}|$ characteristics, respectively. By using a choke structure instead of via holes, the measured result of the reflection characteristic still exhibits a double-resonant frequency at 73.5 GHz and 79 GHz and a broad frequency bandwidth of 9.6 GHz (12.5%) at $|S_{11}| = -15$ dB. The measured insertion loss almost agrees with the simulated result. The measured insertion loss at the center frequency of 76.5 GHz is 0.6 dB. The insertion loss of the transition with the choke structure is approximately 0.2 dB higher than that with via-hole arrangement.

Table 2 shows the performance summary of the state-of-the-art broadband microstrip-to-waveguide transitions.

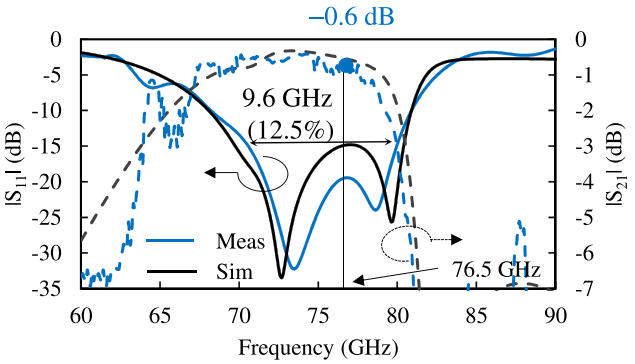

FIGURE 16. Measured and simulated $|S_{11}|$ and $|S_{21}|$ of the broadband microstrip-to-waveguide transition with the choke structure.

TABLE 2. Performance summary of the state-of-the-art microstrip-to-waveguide transitions.

	f_c (GHz)	Reference S_{11} (dB)	Bandwidth (%)	Insertion loss (dB)	Process	WG
[28]	76.5	-15	6.9	0.5	ML	WR-12
[16]	10	-12	35	0.3	quasi-Yagi	WR-90
[20]	60	-10	41	0.58	SIW	WR-15
[21]	35	-15	10.6	0.7	SIW, ML	WR-28
[22]	24	-15	n.a	1.7	SIW, ML	WR-42
[23]	28	-15	16	0.8	SIW, ML	WR-28
[24]	67	-10	45.5	0.5	SIW	WR-15
[25]	32.5	-15	46.5	0.65	SIW	WR-28
This work	76.5	-15	13.8	0.41	ML	WR-12

Although the techniques and design frequencies are different for each study, the fairest comparisons are given to evaluate the effectiveness of this study. The frequency bandwidth of 10.6 GHz at reference $|S_{11}| = -15$ dB is wide, with the waveguide standard of WR-12. The insertion loss of the proposed transition, obtained as 0.41 dB, is also respectable in comparison with that of the other designs. Note that the other designs are quite complex structures because they used both a substrate integrated waveguide (SIW) and a microstrip line (ML) along with the excitation from a larger waveguide standard. Therefore, the advantages of the proposed broadband microstrip-to-waveguide transition have been clearly highlighted.

V. CONCLUSION

A design technique of the multi-transmission mode for a broadband planar microstrip-to-waveguide transition has been proposed. The broadband microstrip-to-waveguide transition works under a combination of the G-CPW mode and parallel plate mode by controlling the positions of two via holes at the input port. A double-resonant frequency and a broad bandwidth of 10.6 GHz (13.8%) were obtained. The measured results of the broadband planar microstrip-to-waveguide transition with via-hole arrangement showed an insertion loss of 0.41 dB at the center frequency of 76.5 GHz. Then, the choke structure was proposed to replace the via-hole arrangement. The choke structure is attractive from an industrial point of view because of its simple structure, low cost, and small assembly tolerance. The measured results of the broadband microstrip-to-waveguide transition with the choke structure exhibited an insertion loss of 0.6 dB at 76.5 GHz. The feasibility of the broadband microstrip-to-waveguide transition was confirmed by the measured performances, and it could be applied in practical millimeter-wave systems.

REFERENCES

[1] P. Wang, Y. Li, L. Song, and B. Vucetic, "Multi-gigabit millimeter wave wireless communications for 5G: From fixed access to cellular networks," *IEEE Commun. Mag.*, vol. 53, no. 1, pp. 168–178, Jan. 2015.

[2] K. Ohata, T. Inoue, M. Funabashi, A. Inoue, Y. Takimoto, T. Kuwabara, S. Shinozaki, K. Maruhashi, K. Hosaya, and H. Nagai, "Sixty-GHz-band ultra-miniature monolithic T/R modules for multimedia wireless communication systems," *IEEE Trans. Microw. Theory Techn.*, vol. 44, no. 12, pp. 2354–2360, Dec. 1996.

[3] T. S. Rappaport, S. Sun, R. Mayzus, H. Zhao, Y. Azar, K. Wang, G. N. Wong, J. K. Schulz, M. Samimi, and F. Gutierrez, "Millimeter wave mobile communications for 5G cellular: It will work!" *IEEE Access*, vol. 1, pp. 335–349, 2013.

[4] J. J. Lynch, K. S. Kona, R. G. Nagele, G. L. Virbila, R. L. Bowen, and M. D. Wetzel, "128 element coded aperture radar at 77 GHz," in *IEEE MTT-S Int. Microw. Symp. Dig.*, Munich, Germany, Apr. 2018, pp. 1–4.

[5] H. Sharifi, H. J. Song, M. Yajima, K. Kona, A. Bekaryan, K. Geary, and I. Bilik, "Semi-transparent and conformal antenna technology for millimeter-wave intelligent sensing," in *IEEE MTT-S Int. Microw. Symp. Dig.*, Munich, Germany, Apr. 2018, pp. 1–4.

[6] S. Hastürkoğlu and S. Lindenmeier, "An automotive antenna set at 26.5 GHz for 5G-mobile communication," in *IEEE MTT-S Int. Microw. Symp. Dig.*, Munich, Germany, Apr. 2018, pp. 1–4.

[7] R. Feger, A. Haderer, and A. Stelzer, "Experimental verification of a 77-GHz synthetic aperture radar system for automotive applications," in *IEEE MTT-S Int. Microw. Symp. Dig.*, Nagoya, Japan, Mar. 2017, pp. 111–114.

[8] M. Murad, J. Nickolaou, G. Raz, J. S. Colburn, and K. Geary, "Next generation short range radar (SRR) for automotive applications," in *Proc. IEEE Radar Conf.*, Atlanta, GA, USA, May 2012, pp. 0214–0219.

[9] D. A. Williams, "Millimetre wave radars for automotive applications," in *IEEE MTT-S Int. Microw. Symp. Dig.*, Albuquerque, NM, USA, vol. 2, Jun. 1992, pp. 721–724.

[10] W. Menzel, D. Pilz, and R. Leberer, "A 77-GHz FM/CW radar front-end with a low-profile low-loss printed antenna," *IEEE Trans. Microw. Theory Techn.*, vol. 47, no. 12, pp. 2237–2241, Dec. 1999.

[11] J. Hirokawa and M. Ando, "Efficiency of 76-GHz post-wall waveguide-fed parallel-plate slot arrays," *IEEE Trans. Antennas Propag.*, vol. 48, no. 11, pp. 1742–1745, Nov. 2000.

[12] A. Mizutani, K. Sakakibara, N. Kikuma, and H. Hirayama, "Grating lobe suppression of narrow-wall slotted hollow waveguide millimeter-wave planar antenna for arbitrarily linear polarization," *IEEE Trans. Antennas Propag.*, vol. 55, no. 2, pp. 313–320, Feb. 2007.

[13] Y. Hayashi, K. Sakakibara, M. Nanjo, S. Sugawa, N. Kikuma, and H. Hirayama, "Millimeter-wave microstrip comb-line antenna using reflection-canceling slit structure," *IEEE Trans. Antennas Propag.*, vol. 59, no. 2, pp. 398–406, Feb. 2011.

[14] S. Sugawa, K. Sakakibara, N. Kikuma, and H. Hirayama, "Low-sidelobe design of microstrip comb-line antennas using stub-integrated radiating elements in the millimeter-wave band," *IEEE Trans. Antennas Propag.*, vol. 60, no. 10, pp. 4699–4709, Oct. 2012.

[15] H.-W. Yao, A. Abdelmonem, J.-F. Liang, and K. A. Zaki, "Analysis and design of microstrip-to-waveguide transitions," *IEEE Trans. Microw. Theory Tech.*, vol. 42, no. 12, pp. 2371–2379, Dec. 1994.

[16] N. Kaneda, Y. Qian, and T. Itoh, "A broad-band microstrip-to-waveguide transition using quasi-Yagi antenna," *IEEE Trans. Microw. Theory Tech.*, vol. 47, no. 12, pp. 2562–2567, Dec. 1999.

[17] D. Deslandes and K. Wu, "Integrated microstrip and rectangular waveguide in planar form," *IEEE Microw. Wireless Compon. Lett.*, vol. 11, no. 2, pp. 68–70, Feb. 2001.
[18] Y.-C. Leong and S. Weinreb, "Full band waveguide-to-microstrip probe transitions," in *IEEE MTT-S Int. Microw. Symp. Dig.*, Anaheim, CA, USA, vol. 4, Jun. 1999, pp. 1435–1438.
[19] W. Grabherr, B. Huder, and W. Menzel, "Microstrip to waveguide transition compatible with MM-wave integrated circuits," *IEEE Trans. Microw. Theory Techn.*, vol. 42, no. 9, pp. 1842–1843, Sep. 1994.
[20] Y. Li and K.-M. Luk, "A broadband V-band rectangular waveguide to substrate integrated waveguide transition," *IEEE Microw. Wireless Compon. Lett.*, vol. 24, no. 9, pp. 590–592, Sep. 2014.
[21] X. Dai, "An integrated millimeter-wave broadband microstrip-to-waveguide vertical transition suitable for multilayer planar circuits," *IEEE Microw. Wireless Compon. Lett.*, vol. 26, no. 11, pp. 897–899, Nov. 2016.
[22] A. Mozharovskiy, S. Churkin, A. Arternenko, and R. Maslcnnikov, "Wideband probe-type waveguide-to-microstrip transition for 28 GHz applications," in *Proc. 48th Eur. Microw. Conf. (EuMC).*, Madrid, Spain, Sep. 2018, pp. 113–116.
[23] E. Hassan, M. Berggren, B. Scheiner, F. Michler, R. Weigel, and F. Lurz, "Design of planar microstrip-to-waveguide transitions using topology optimization," in *Proc. IEEE Radio Wireless Symp. (RWS).*, Orlando, FL, USA, Jan. 2019, pp. 1–3.
[24] I. Mohamed and A. Sebak, "Broadband transition of substrate-integrated waveguide-to-air-filled rectangular waveguide," *IEEE Microw. Wireless Compon. Lett.*, vol. 28, no. 11, pp. 966–968, Nov. 2018.
[25] J. Dong, Y. Liu, H. Lin, and T. Yang, "Low loss and broadband transition between substrate integrated waveguide and rectangular waveguide," *Int. J. RF Microw. Comput. Aided Eng.*, vol. 26, no. 1, pp. 54–61, 2016.
[26] N. Dib and A. Omar, "Analysis of grounded coplanar waveguide fed patches and waveguides," *IEEE Antennas Propag. Soc. Int. Symp.*, Montreal, QC, Canada, vol. 4, Jul. 1997, pp. 2530–2533.
[27] H. Iizuka, T. Watanabe, K. Sato, and K. Nishikawa, "Millimeter-wave microstrip line to waveguide transition fabricated on a single layer dielectric substrate," *IEICE Trans. Commun.*, vol. E85-B, no. 6, pp. 1169–1177, Jun. 2002.
[28] H. Iizuka, K. Sakakibara, and N. Kikuma, "Millimeter-wave transition from waveguide to two microstrip lines using rectangular patch element," *IEEE Trans. Microw. Theory Techn.*, vol. 55, no. 5, pp. 899–905, May 2007.
[29] K. Seo, K. Sakakibara, and N. Kikuma, "Transition from waveguide to two microstrip lines with slot radiators in the millimeter-wave band," *IEICE Trans. Commun.*, vol. E94-B, no. 5, pp. 1184–1193, May 2011.
[30] K. Murase, K. Sakakibara, N. Kikuma, and H. Hirayama, "Design of via-less planer microstrip-to-waveguide transition with choke structure," in *Proc. Int. Symp. Antennas Propag. (ISAP)*, Nagoya, Japan, Oct./Nov. 2012, pp. 267–270.
[31] T. T. Nguyen, K. Sakakibara, and N. Kikuma, "Bandwidth extension of planar microstrip-to-waveguide transition by via-hole arrangement," in *Proc. Int. Symp. Antennas Propag. (ISAP)*, Busan, South Korea, Oct. 2018, pp. 1–2.
[32] *Ansoft Corporation, Version 17.2*, HFSS, Pittsburgh, PA, USA, 2017.
[33] J. Dunsmore, "Gating effects in time domain transforms," in *Proc. 72nd ARFTG Microw. Meas. Symp.*, Portland, OR, USA, Dec. 2008, pp. 1–8.

NGUYEN THANH TUAN was born in Hanam, Vietnam, in August 1991. He received the B.S. degree in electronics and telecommunication from the Hanoi University of Science and Technology, Hanoi, Vietnam, in 2014, and the M.S. degree in electronic systems from University Technology Malaysia, in 2017. He is currently pursuing the Ph.D. degree with the Department of Electrical and Mechanical Engineering, Nagoya Institute of Technology, Nagoya, Japan. His current research interests include the beamforming networks for millimeter-wave antennas and microstrip array antennas.

KUNIO SAKAKIBARA (M'94–SM'06) was born in Aichi, Japan, in 1968. He received the B.S. degree in electrical and computer engineering from the Nagoya Institute of Technology, Nagoya, Japan, in 1991, and the M.S. and D.E. degrees in electrical and electronic engineering from the Tokyo Institute of Technology, Tokyo, Japan, in 1993 and 1996, respectively.

From 1996 to 2002, he was with Toyota Central R & D Labs, Inc., Nagakute, where he was involved in the development of antennas for automotive millimeter-wave radar systems. From 2000 to 2001, he was a Guest Researcher with the Department of Microwave Techniques, University of Ulm, Ulm, Germany. In 2002, he joined the Nagoya Institute of Technology as a Lecturer. Since 2004, he has been an Associate Professor with the Nagoya Institute of Technology, where he became a Professor, in 2012. His current research interests include millimeter-wave antennas and feeding circuits.

NOBUYOSHI KIKUMA (M'83–SM'03) was born in Ishikawa, Japan, in 1960. He received the B.S. degree in electronic engineering from the Nagoya Institute of Technology, Japan, in 1982, and the M.S. and Ph.D. degrees in electrical engineering from Kyoto University, Japan, in 1984 and 1987, respectively.

From 1987 to 1988, he was a Research Associate with Kyoto University. In 1988, he joined the Nagoya Institute of Technology, where he has been a Professor, since 2001. His current research interests include adaptive and signal processing arrays and multipath propagation analysis, mobile and indoor wireless communication, and electromagnetic field theory. He was a recipient of the 4th Telecommunications Advancement Foundation Award, in 1989.